Journal of Physics: Conference Series **2919** (2024) 012019 doi:10.1088/1742-6596/2919/1/012019

Optimization of leptonic CP violation search using baseline configurations in neutrino oscillation experiments

Ankur Nath[a], **Cao Van Son**[b], **Jennifer Thomas**[c], **Quyen Phan To**[b,d]

[a]Namrup College, Assam, India, ZIP 786623
[b]Institute For Interdisciplinary Research in Science and Education (IFIRSE),Vietnam
[c]University College London, England
[d]Graduate University of Science and Technology, VAST, Hanoi, Vietnam

E-mail: anath.namrup@gmail.com

Abstract. One of the fundamental goals of the neutrino program over the next decade will be to look for leptonic CP violation and precisely determine its magnitude. Neutrino oscillation measurements are frequently conducted with a near-site detector for constraining the flux and neutrino interaction models and a far-site monolithic massive detector for measuring the oscillated spectrum pattern. In this work, we present an investigation of an alternative experimental configuration to improve the CP violation measurement sensitivity by using multiple sub-detectors while keeping the overall detector mass constant and placing them at different baselines. The study makes use of neutrino beams from the T2HK, DUNE and ESSνSB experiments. It is found that the coverage of true δ_{CP} values that can be explored with $\geq 5\sigma$ C.L. improves significantly after deploying multiple far detectors, instead of the conventional single far-detector technique.

1 Introduction

Neutrino evolution equation in matter, in terms of flavour eigenstates, is given by

$$i\frac{d}{dx}\nu_\alpha = \mathcal{H}(x)\nu_\alpha$$

where $\nu_\alpha(\alpha = e, \mu, \tau)$ iS the amplitude for α flavour and $\mathcal{H}(x)$ is the hamiltonian in matter[1]. It reads as as the function of x, the position along the neutrino trajectory and is given by

$$\mathcal{H}(x) = U\, diag\Big[0, \frac{m_{21}^2}{2E}, \frac{m_{31}^2}{2E}\Big]U^\dagger + diag\Big[V_{CC}(x), 0, 0\Big] \tag{1}$$

$V_CC(x) = \sqrt{G_F}N_e(x)$ is the matter potential, where G_F is the Fermi constant, $N_e(x)$ is the electron number density at x. U is the 3×3 Pontecorvo-Maki-Nakagawa-Sakata (PMNS) matrix[2, 3], given by

$$U = \begin{bmatrix} c_{12}c_{13} & s_{12}c_{13} & s_{13}e^{-i\delta_{CP}} \\ -s_{12}c_{23} - c_{12}s_{13}s_{23}e^{i\delta_{CP}} & c_{12}c_{23} - s_{12}s_{13}s_{23}e^{i\delta_{CP}} & c_{13}s_{23} \\ s_{12}s_{23} - c_{12}s_{13}c_{23}e^{i\delta_{CP}} & -c_{12}s_{23} - s_{12}s_{13}c_{23}e^{i\delta_{CP}} & c_{13}c_{23} \end{bmatrix} P_m, \tag{2}$$

where, $c_{ij} = \cos\theta_{ij}$, $s_{ij} = \sin\theta_{ij}$ (for *i,j = 1,2,3*), and $P_m = diag(1, i\rho_1, i\rho_2)$ denotes the diagonal Majorana phase matrix, which does not have any effect on the neutrino oscillations.

Table 1: Oscillation parameters used for the sensitivity analysis, taken from Ref. [4].

Parameter	$\sin^2\theta_{12}$	$\sin^2\theta_{13}$	$\sin^2\theta_{23}$	Δm^2_{21} (10^{-5})	$\Delta m^2_{32}(10^{-3})$
Best Fit	0.303	0.02203	0.572	7.41 eV^2	2.511 eV^2

The unsolved problems in neutrino oscillation physics include leptonic CP violation (CPV), neutrino mass hierarchy (MH), which refers to the order of the three mass eigenvalues of neutrino mass eigenstates (whether *normal* i.e. $m_1 < m_2 < m_3$ or *inverted* i.e. $m_3 < m_1 < m_2$?) and whether the mising angle θ_{23} prefers maximal mixing i.e. $\frac{\pi}{4}$, higher octant ($> \frac{\pi}{4}$) or lower octant ($< \frac{\pi}{4}$). The global fit of the oscillation parameters, assuming normal mass ordering is given in Table 1. Conventionally, we employ a single far detector (FD) for oscillation analysis and a near detector (ND) to put constraints on the uncertainties of flux and cross-sections, thereby addressing the unknowns *viz.* CP violation, mass ordering, and θ_{23} precision. What if we can place multiple detectors as array of FDs, can it enhance the physics potential of an experiment to above questions? One such approach was considered in the CHerenkov detectors In mine PitS (CHIPS)[5] experiment where modules of water cherenkov detectors were placed in a flooded mine pit in northern Minnesota, 7 mrad off-axis from the existing NuMI beam. In this study, we consider arrays of far detectors (FDs) instead of single FD technique to optimize CPV search in LBNEs. In section 2, we present the motivation of the work, and specify the experimental details. The simulation method is discussed and the results are presented in section 3. The discussion and future scope of the study are mentioned in sections 4.

2 Motivation and Experimental Specifications

Accelerator-based long baseline (A-LBL) experiments offer the unique opportunity of testing the leptonic CP Violation phenomenon by measuring the difference of the appearance of the electron neutrino (ν_e) and anti-neutrino ($\bar{\nu}_e$) from muon neutrino (ν_μ) and muon anti-neutrino ($\bar{\nu}_\mu$) respectively from the source. T2K of Japan and NOνA are the ongoing A-LBLs. Analytically[6], CPV is given by,

$$A^{\mu e}_{CP} = \sin\theta_{12}\cos\theta_{12}\sin\theta_{23}\cos\theta_{23}\sin\theta_{13}\cos^2\theta_{13}\sin\delta_{CP}\sin\frac{\Delta m^2_{21}L}{4E}\sin\frac{\Delta m^2_{32}L}{4E}\sin\frac{\Delta m^2_{31}L}{4E}$$

From the above equation, it is understood that CPV measurement is sensitive to all the oscillation parameters. Although other parameters are well measured and found to be non-zero, we still don't know the value of δ_{CP}. The necessary condition for observation of leptonic CPV is non-zero values of $\sin\delta_{CP}$ *i.e.* exclusion of CP conserving values 0 and $\pm\pi$. Recent data of T2K gives a hint on CP violations in leptons[7]. However, future measurements with larger datasets are required to precisely answer this question. In our work, we consider the specifications of that of the upcoming experiments Tokai-to-HyperKamiokande (T2HK)[8], Deep Underground Neutrino Experiment (DUNE)[9] and European Spallation Source neutrino Super Beam (ESSνSB)[10] to reconsider their baselines to test our novel concept of optimizing CP violation using baseline configurations. The schematic geographical locations and the experimental specifications of the these considered experiments are given in Figure 1 and Table 2 respectively. The event rates, event spectra and sensitivities to exclude CP conserving values of the experiments are validated as in Ref. [8, 11, 10] respectively.

Figure 1: Geographical locations of the considered A-LBL experiments: T2HK (*left*), DUNE (*centre*) and ESSνSB (*right*).

In this work, we consider two-FDs, three-FDs arrays instead of the conventional one FD option, while keeping the total combined fiducial mass of the detectors equal to that of the one-FD set-up of the considered experiments. The motivation for considering multiple FDs, in the case of DUNE is shown in Figure 2. In the top figures, bi-event plots of ν_e versus $\bar{\nu}_e$ appearance events are obtained, for both NO and IO, using DUNE FD fluxes for baselines of 1300 km (left) and 750 km (right). As δ_{CP} is unknown, the plots are generated for the allowed range of $[\pi, -\pi]$, leading to the ellipses. Comparing the left and right bi-event plots, two observations can be made: (i) As the flux $\Phi(E, L) \propto \frac{1}{L^2}$, higher ν_e and $\bar{\nu}_e$ appearance events are obtained for L=750 km; and (ii) the ellipses for a particular value of θ_{23} (right plot) overlap on each other. The MO sensitivity plots to reject the wrong ordering are shown in the *right bottom* plot for various combination of baselines. It is evident from the *blue* (L=750 km) and *black* curve (L=1300 km) that the ability to discriminate between NO and IO at a higher confidence level is compromised for the smaller baseline. However, in the case where we consider set-ups of two FDs simultaneously at 750km and 1300km, along with a ND, the sensitivity to MO is restored well above 5σ C.L. (*see orange plot*). The combination of baselines selection for arrays of FDs for each experiment considered in our simulation is given in Table 3.

Table 2: List of Experimental Specifications of the considered experiments ($^{\dagger}(\nu + \bar{\nu})$ runtime.)

Parameters	T2HK	DUNE	ESSνSB
Baseline:	295 km	1284.9 km	360 km
Beam Power:	1.3 MW	1.2 MW	5 MW
Detector Target	Water Cherenkov	Liquid Argon-TPC	Water Cherenkov
Detector Volume:	187 kton	40 (20) kton	538 kton
Runtime:	(2.5+7.5)† years	(5+5)† years	(5+5)† years

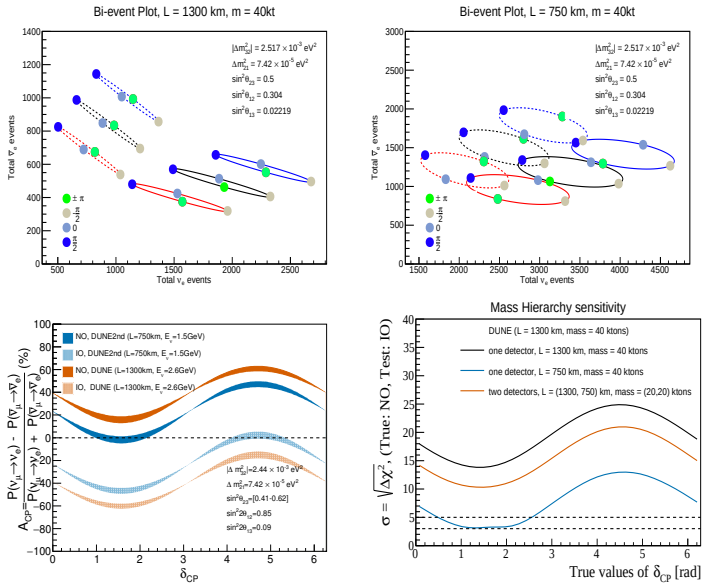

Figure 2: Consideration of arrays of two and three far detectors for the DUNE experiment: ***Top:*** Bi-event rates for L= 1300 km (750 km) in the left (right) plot corresponding to DUNE experiment. Solid (dashed) ellipses represents NO (IO). ***Bottom:*** CP Asymmetry (left) and MH sensitivity (right) as function of δ_{CP}.

Table 3: DUNE, HK and ESSνSB FDs array: Baseline and mass distribution

FD Set-up	**Detector Mass**	**FD Set-up**	**Detector Mass**
DUNE (1300 km)	40 ktons	**HK** (295 km)	187 ktons
(1300,1000) km	(20,20) ktons	(295,265) km	(187,187) ktons
(1300,750) km	(20,20) ktons	(295,325) km	(187,187) ktons
(1300,1000,750)	(13.3,13.3,13.3) ktons	(295,265,325)	(124.7,124.7,124.7) ktons

FD Set-up	**Detector Mass**
ESS (360 km)	538 ktons
(360,450) km	(269,269) ktons
(360,540) km	(269,269) ktons
(360,450,540)	(179.3,179.3,179.3) ktons

3 Simulation Technique and Results

The number of final neutrino events at the detector is given by:

$$N_{\nu_\beta} \propto \overbrace{\Phi_\alpha(E)}^{Production} \times \underbrace{\frac{1}{L^2} P_{(\nu_\alpha \to \nu_\beta)}(E, L, \rho; \theta_{12}, \theta_{13}, \theta_{23}, \Delta m^2_{21}, \Delta m^2_{31}, \delta_{CP})}_{Propagation} \times \overbrace{\sigma(E)}^{Interaction} \times \underbrace{\epsilon}_{Detection} \tag{3}$$

where, $\alpha = \nu_\mu$ ($\bar{\nu}_\mu$) and $\beta = \nu_e$ ($\bar{\nu}_e$) flavors in neutrino (anti-neutrino) modes. In the above expression, N_{ν_β} is the number of final neutrino flavor, which is ν_μ ($\bar{\nu}_\mu$) and ν_e ($\bar{\nu}_e$) events in disappearance and appearance channels, respectively, in neutrino (anti-neutrino) mode. Φ_α(E) is the flux of initial initial flavor (ν_μ and $\bar{\nu}_\mu$) as a function of true neutrino energy produced at the source. $P(\nu_\alpha \to \nu_\beta)$ or $P_{\alpha\beta}$ is the oscillation probability of ν_α to the final

Table 4: Energy window and Systematic uncertainties of signal and background events for the considered experiments.

Experiments	Energy	window (GeV)	Signal	errors	Background	errors
	App	*Dis*	*App*	*Dis*	*App*	*Dis*
T2HK	0.1-2.0	0.2-3.0	$\sim 4.5\%$	$\sim 4\%$	10%	10%
DUNE	0.5-18	0.5-18	2%	5%	5%	5%
ESSνSB	0.1-1.0	0.1-1.0	5%	5%	5%	5%

neutrino flavor (ν_β) at the detector after travelling a baseline length of L (in km). In our work, four oscillation channels $P_{\mu\mu}$, $P_{\bar{\mu}\bar{\mu}}$ (i.e. disappearance of ν_μ and $\bar{\nu}_\mu$), $P_{\mu e}$ and $P_{\bar{\mu}\bar{e}}$ (i.e. appearance of ν_e and $\bar{\nu}_e$) are considered for simulation. $\sigma(E)$ is the cross-section of the final flavor neutrino at the detector and ϵ is the detection efficiencies of the ν_β.

We use the General Long Baseline Experiment Simulator (GLoBES) [12, 13] to perform the simulation work. In the measurement of statistical significance to exclude CP conserving values $(0, \pm\pi)$, we assume the test values of $\delta_{CP} = 0, \pm\pi$ and compute the $\Delta\chi^2$ for any true δ_{CP} in the allowed range of $[-\pi, \pi]$ given by,

$$\Delta\chi^2(\delta_{CP}^{true}) \sim \min\left(\chi^2_{total}(\delta_{true}) - \chi^2_{total}(\delta_{CP}^{test} = 0, \pm\pi)\right)$$

For the minimization of χ^2 over the MH options, we consider two cases:
(i) MH is known and normal, or (ii) MH is unknown.

3.1 Results

In Figure 3 and 4, the fraction of true δ_{CP} values that can be explore with at least 3σ C.L. to exclude CP conserving values ($\delta_{CP} = 0, \pm\pi$) are shown as function of baselines (in km). The black (blue) curves represent for the case when the mass hierarchy is known (unknown). Figure 5 shows the CPV sensitivity to reject CP conserving values ($\delta_{CP} = 0, \pm\pi$) as function of true δ_{CP} values for arrays of 2-FDs of (295, 295), (295, 265), (295, 325) and 3-FDs array of (265, 295, 325) in kms, using HyperKamiokande flux profile. The top plots of figure 6 show the CPV sensitivity for arrays of 2-FDs of (1300, 750), (1300, 1000) and 3-FDs of (1300, 1000, 750) in kms, using DUNE flux profiles. In case of ESSνSB, we consider baseline (in *km*) combination of (360, 450), (360, 540) for arrays of 2-FDs and (360, 450, 540) for an array of 3-FDs and CPV sensitivity to reject $\delta_{CP} = 0, \pm\pi$ is shown in the bottom plots.

The energy window for appearance and disappearance samples of different baseline configurations considered for the statistical analyses is given in Table 3. The systematic parameters are the uncertainties associated with the signal and background events of the appearance and disappearance samples as given in the table. In figure 5, the *top* (*bottom*) figures are the CPV sensitivity plots for the case when the systematics are uncorrelated (correlated). When the systematics are uncorrelated, the signal and background errors for the appearance and disappearance samples for various FD combinations in neutrino and anti-neutrino modes are taken as in Table 4. For the case when are systematics are correlated in the arrays of FDs, the signal and background errors of the first FD is taken as in Table 4. However, the 2nd or (and) the 3rd detector(s) for an array of 2 (3) FDs, we consider the signal and background uncertainties of 1% only. The reason behind this assumption is that for a particular flux profiles, the FDs in an array have the same detector target which, for instance, is water in case of HK experiment. As such, the uncertainties arising due to flux and cross-section measurements cancel out. This gives a boost to the CPV sensitivity measurement.

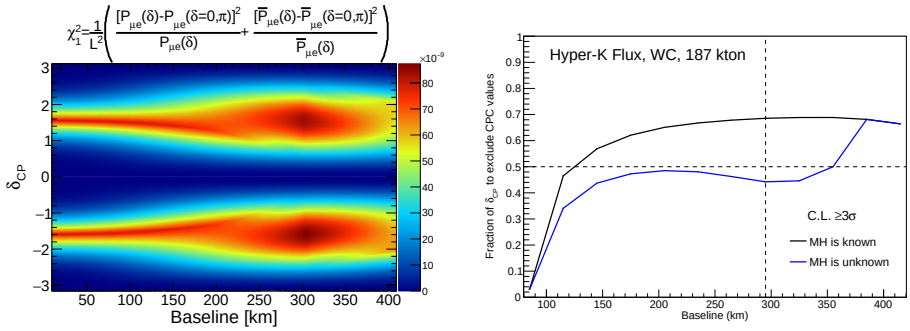

Figure 3: *Left*: $L - \delta_{CP}$ 2D plot showing the coverage of δ_{CP} given a far detector is placed at a particular baseline. In this plot, the neutrino energy is fixed at $E = 0.6$ GeV. The χ^2 calculation includes convolution of oscillation probability and change of flux with baseline respresented by the term $\frac{1}{L^2}$. *Right:* Fraction of true δ_{CP} that can be explored with atleast 3σ C.L. to exclude CPC values, as a function of baseline (in km), using HK FD flux.

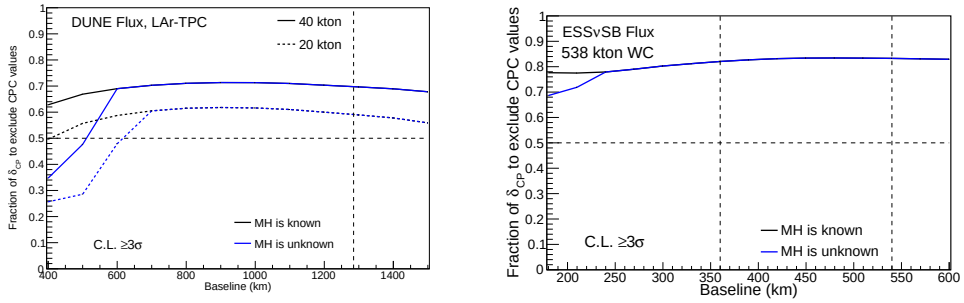

Figure 4: Fraction of true δ_{CP} that can be explored with atleast 3σ C.L. to exclude CPC values, as a function of baseline (in km), using DUNE (ESSνSB) FD flux is shown in the lef (right) plot.

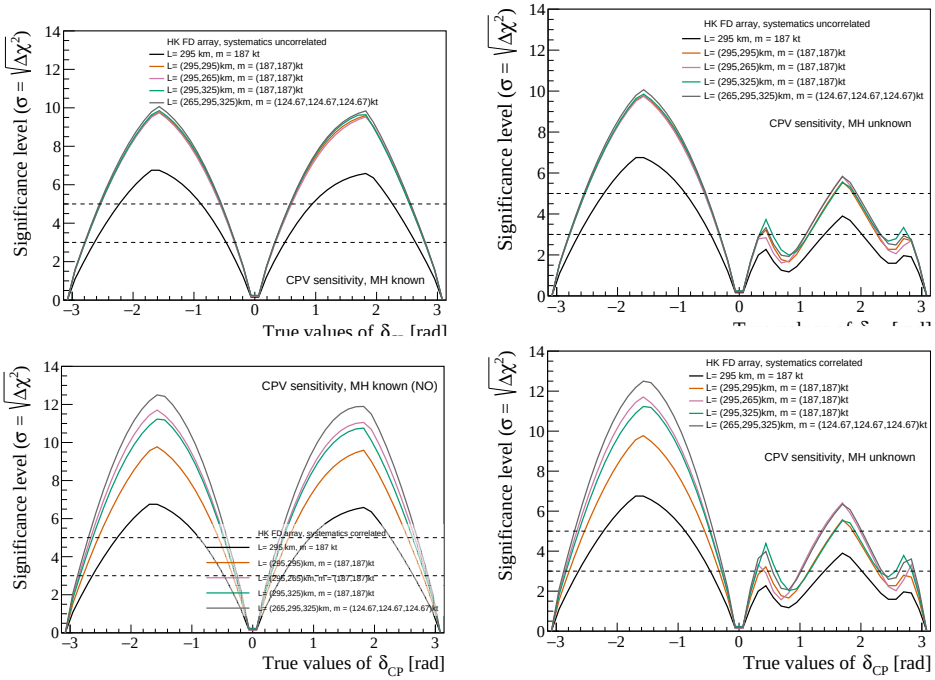

Figure 5: CPV sensitivity for Hyper-Kamiokande 2-FDs and 3-FDs arrays: In the *right* (*left*) plots, mass ordering is considered to be unknown (known and is normal). The signal and background errors are kept uncorrelated (correlated) among the FDs, as shown in the *top* (*bottom*) plots.

Table 5: Fractional region of true δ_{CP} (in %) that can be explored with 5σ or higher significance when the *mass hierarchy is known (NO)*, for arrays of far detectors using Hyper-Kamiokande flux.

HK array (km)	**(295,295)**	(295,265)	(265, 295)	(265, 295, 325)
Uncorrelated	**62.4**	62.1	62.7	63.5
Correlated		69.5	67.9	72.2

Table 6: Fractional region of true δ_{CP} (in %) that can be explored with 5σ or higher significance when the *mass hierarchy is unknown, for arrays of far detectors using DUNE flux.*

DUNE array (km)	**1300**	(1300,1000)	(1300, 750)	(750, 1000, 1300)
Uncorrelated	**46**	50.4	50.6	52.7
Correlated		52.4	52.5	54.3

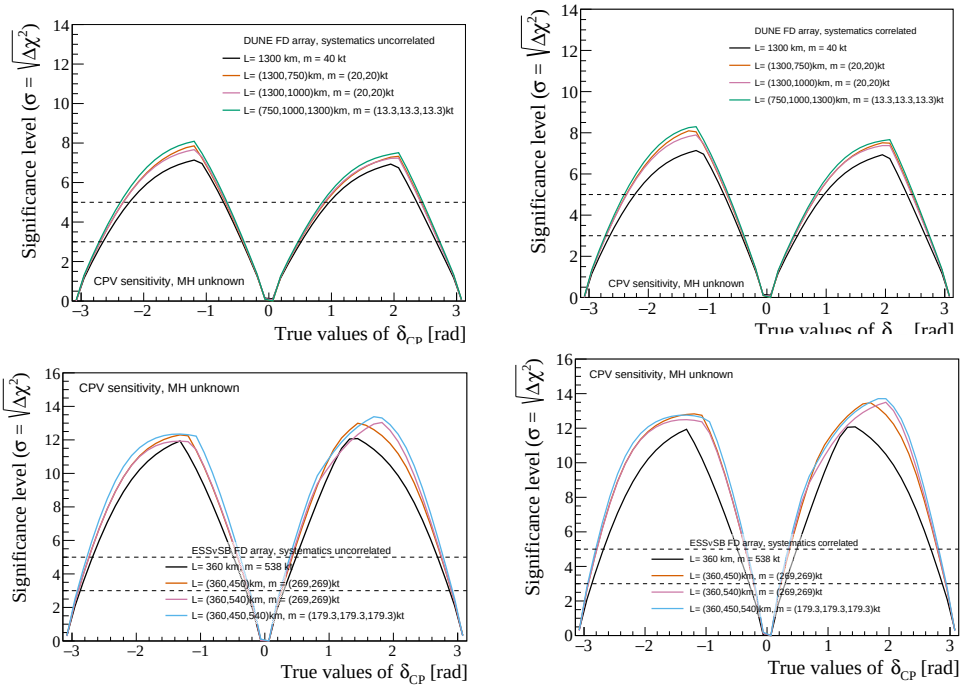

Figure 6: CPV sensitivity for DUNE (top) and ESSνSB (bottom) 2-FDs and 3-FDs arrays: The signal and background errors are kept uncorrelated (correlated) among the FDs, as shown in the *top* (*bottom*) plots. Mass ordering is assumed to be known in each case.

Table 7: Fractional region of true δ_{CP} (in %) that can be explored with 5σ or higher significance when the *mass hierarchy is unknown*, for arrays of far detectors using ESSνSB flux.

ESSνSB array (km)	**360**	(360,450)	(360, 540)	(360, 450, 540)
Uncorrelated	**69.9**	73.6	74.0	75.9
Correlated		77.2	77.4	78.7

Tables 5, 6 and 7 shows the fraction of true δ_{CP} values that can be explored with $5\sigma$of higher significance for the cases when the systematics are uncorrelated and correlated. It is found that in the coverage of true δ_{CP} values that can be explored with ≥ 5 C.L. improves significantly with an increase of about $(12.6 - 18.0)\%$ after deploying multiple FDs w.r.t. that of the conventional single-FD technique.

4 Discussion and Future Scope

Currently, accelerator-based long baseline experiments use a far detector to perform the oscillation analyses and a near detector to constrain the flux and cross-section uncertainties. Through this work, we investigate the scope of using multiple FDs, while keeping the the combined fiducial volume of the FDs equal to that of the conventional single FD set-up. Initially, the fraction of true δ_{CP} values to exclude CP conserving values as a function of baselines is tested in order to consider the locations for the second and third far detectors. Due to smaller baseline and smaller matter effects for the case using HyperK flux, the sensitivity is effected when the mass ordering is unknown. For experiments with longer baselines like DUNE and ESSνSB, the coverage of true δ_{CP} values is not affected whether the mass ordering is known or unknown. It is further observed that employing arrays of far detectors (FDs) enhances the coverage of the allowed true δ_{CP} regions to exclude the CPC values. Particularly, CPV sensitivity shows a great boost when we consider correlation among the systematics of the different FDs. With this novel idea, the coverage of true δ_{CP} values that can be explored with ≥ 5 C.L. improves significantly with an increase of about $(12.6 - 18.0)\%$. With the proposed set-up, relatively large statistics from multiple FDs with high power beam (eg. 5MW for ESSνSB, $\sim$1 MW for T2HK and DUNE) can be achieved. The correlation in the flux, cross-section and detector response constrain themselves via the multi-detector data fit and result in improved sensitivity to CPV measurements. However, it is to be emphasized that more realistic approach to establish the correlation among the flux profiles, signal and background event rates of the FDs is required. Moreover, effect on CPV sensitivity using an array of FDs and without a near detector should also be studied. This concept can be helpful while constructing upcoming accelerator-based experiments to arrange an array of FDs instead of just one.

Acknowledgement
Phan To Quyen was funded by the Master, PhD Scholarship Programme of Vingroup Innovation Foundation (VINIF), code VINIF.2023.TS.095. The research of Ankur Nath is funded by the National Foundation for Science and Technology Development (NAFOSTED) of Vietnam under Grant No. 103.99-2023.144. Ankur Nath thanks International Centre for Interdisciplinary Science and Education (ICISE), Quy Nhon, Vietnam for the the funding of this research with the neutrino group at Institute For Interdisciplinary Research in Science and Education (IFIRSE), Quy Nhon, Vietnam.

References

[1] Nunokawa H, Parke S, Valle JW. CP violation and neutrino oscillations. Progress in Particle and Nuclear Physics. 2008;60(2):338-402.

[2] Pontecorvo B. Inverse *beta* processes and nonconservation of lepton charge. Zhur Eksptl' i Teoret Fiz. 1958;34.

[3] Maki Z, Nakagawa M, Sakata S. Remarks on the unified model of elementary particles. Progress of Theoretical Physics. 1962;28(5):870-80.

[4] Esteban I, González-García MC, Maltoni M, Schwetz T, Zhou A. The fate of hints: updated global analysis of three-flavor neutrino oscillations. Journal of High Energy Physics. 2020;2020(9):1-22.

[5] Pfutzner MM. Sensitivity study and first prototype tests for the CHIPS neutrino detector R&D program. UCL (University College London); 2018.

[6] Barger V, Whisnant K, Phillips R. CP nonconservation in three-neutrino oscillations. Physical Review Letters. 1980;45(26):2084.

[7] Constraint on the matter–antimatter symmetry-violating phase in neutrino oscillations. Nature. 2020;580(7803):339-44.

[8] proto Collaboration HK, Abe K, Abe K, Ahn S, Aihara H, Aimi A, et al. Physics potentials with the second Hyper-Kamiokande detector in Korea. Progress of Theoretical and Experimental Physics. 2018;2018(6):063C01.

[9] Abi B, Acciarri R, Acero MA, Adamov G, Adams D, Adinolfi M, et al. Volume I. introduction to DUNE. Journal of instrumentation. 2020;15(08):T08008.

[10] Alekou A, Baussan E, Bhattacharyya A, Kraljevic NB, Blennow M, Bogomilov M, et al. The European Spallation Source neutrino super-beam conceptual design report. The European Physical Journal Special Topics. 2022;231(21):3779-955.

[11] Abi B, Acciarri R, Acero M, Adamov G, Adams D, Adinolfi M, et al. Experiment simulation configurations approximating DUNE TDR. arXiv preprint arXiv:210304797. 2021.

[12] Huber P, Kopp J, Lindner M, Rolinec M, Winter W. GLoBES: general long baseline experiment simulator. Computer physics communications. 2007;177(5):439-40.

[13] Huber P, Kopp J, Lindner M, Rolinec M, Winter W. New features in the simulation of neutrino oscillation experiments with GLoBES 3.0:(General Long Baseline Experiment Simulator). Computer Physics Communications. 2007;177(5):432-8.